Developmental Cell
Article

Regulation of Early Wave of Germ Cell Apoptosis and Spermatogenesis by Deubiquitinating Enzyme CYLD

Ato Wright,[1,2] William W. Reiley,[1,3] Mikyoung Chang,[1,2] Wei Jin,[1] Andrew Joon Lee,[1,2] Minying Zhang,[1,2] and Shao-Cong Sun[1,2,*]
[1]Department of Microbiology and Immunology, Pennsylvania State University College of Medicine, 500 University Drive, Hershey, PA 17033, USA
[2]Present address: Department of Immunology, The University of Texas MD Anderson Cancer Center, 7455 Fannin Street, Box 902, Houston TX 77030, USA.
[3]Present address: Trudeau Institute, Inc., 154 Algonquin Ave, Saranac Lake, NY 12983, USA.
*Correspondence: ssun@mdanderson.org
DOI 10.1016/j.devcel.2007.09.007

SUMMARY

Spermatogenesis involves an early wave of germ cell apoptosis, which is required for maintaining the balance between germ cells and supporting Sertoli cells. However, the signaling mechanism regulating this apoptotic event is poorly defined. Here we show that genetic deficiency of *Cyld*, a recently identified deubiquitinating enzyme, attenuates the early wave of germ cell apoptosis and causes impaired spermatogenesis in mice. Interestingly, the loss of CYLD in testicular cells leads to activation of the transcription factor NF-κB and aberrant expression of antiapoptotic genes. We further show that CYLD negatively regulates a ubiquitin-dependent NF-κB activator, RIP1. CYLD binds to RIP1 and inhibits its ubiquitination and signaling function. These findings establish CYLD as a pivotal deubiquitinating enzyme (DUB) that regulates germ cell apoptosis and spermatogenesis and suggest an essential role for CYLD in controlling the RIP1/NF-κB signaling axis in testis.

INTRODUCTION

Spermatogenesis is a tightly controlled biological process in which male germ stem cells undergo sequential phases of changes in the seminiferous tubules to become mature spermatozoa (de Kretser et al., 1998). In the initial phase, spermatogonial stem cells undergo mitotic divisions and differentiate into spermatocytes, which then enter the second phase and undergo meiosis to become haploid spermatids. In the final phase, spermatids differentiate into elongating spermatids and are subsequently transferred into the lumen of epididymis to become spermatozoa. A hallmark of spermatogenesis is the involvement of an early wave of germ cell apoptosis, which is thought to function in keeping a proper balance between germ cells and supporting Sertoli cells (Print and Loveland, 2000; Rodriguez et al., 1997). Deregulation of this early phase of apoptosis can cause aberrant germ cell differentiation during the late stages and result in impaired spermatogenesis (Coultas et al., 2005; Furuchi et al., 1996; Print et al., 1998; Rodriguez et al., 1997; Russell et al., 2002). Despite the extensive cell biological studies, the signaling mechanisms that control the different phases of spermatogenesis are still poorly defined.

An emerging mechanism of cell signaling that regulates diverse biological processes is protein ubiquitination (Haglund and Dikic, 2005). In addition to its well-known role in mediating protein degradation, ubiquitination regulates receptor endocytosis, protein-protein interaction, and other molecular events involved in signal transduction. Protein ubiquitination is a reversible process that is catalyzed by ubiquitin conjugating enzymes and counter-regulated by a family of cysteine proteases known as deubiquitinating enzymes (DUBs) (Nijman et al., 2005). The ubiquitin conjugating enzymes have been extensively studied, but the knowledge of the DUBs is currently quite limited. Recently, a new DUB, CYLD, was identified as a tumor suppressor that is mutated in cylindromatosis, a predisposition of tumors of skin appendages (Bignell et al., 2000). The cylindromatosis patients carry heterozygous mutation of the *Cyld* gene, with loss of heterozygosity occurring in tumor cells. The heterozygous nature of *Cyld* mutations precluded the study of its physiological functions in human patients, but recent work using animal models suggests an important role for CYLD in regulating immune function as well as tumorigenesis (Lim et al., 2007; Massoumi et al., 2006; Reiley et al., 2006, 2007; Zhang et al., 2006). Furthermore, in vitro studies reveal that overexpressed CYLD inhibits the lysine 63 (K63)-linked polyubiquitination of TNF receptor-associated factors (TRAFs) and the regulatory subunit of IκB kinase (IKK) (Brummelkamp et al., 2003; Kovalenko et al., 2003; Trompouki et al., 2003). The K63-linked protein ubiquitination has been implicated as an important mechanism mediating signal transduction, including activation of the transcription factor NF-κB (Chen, 2005). How CYLD regulates protein ubiquitination and signal transduction under

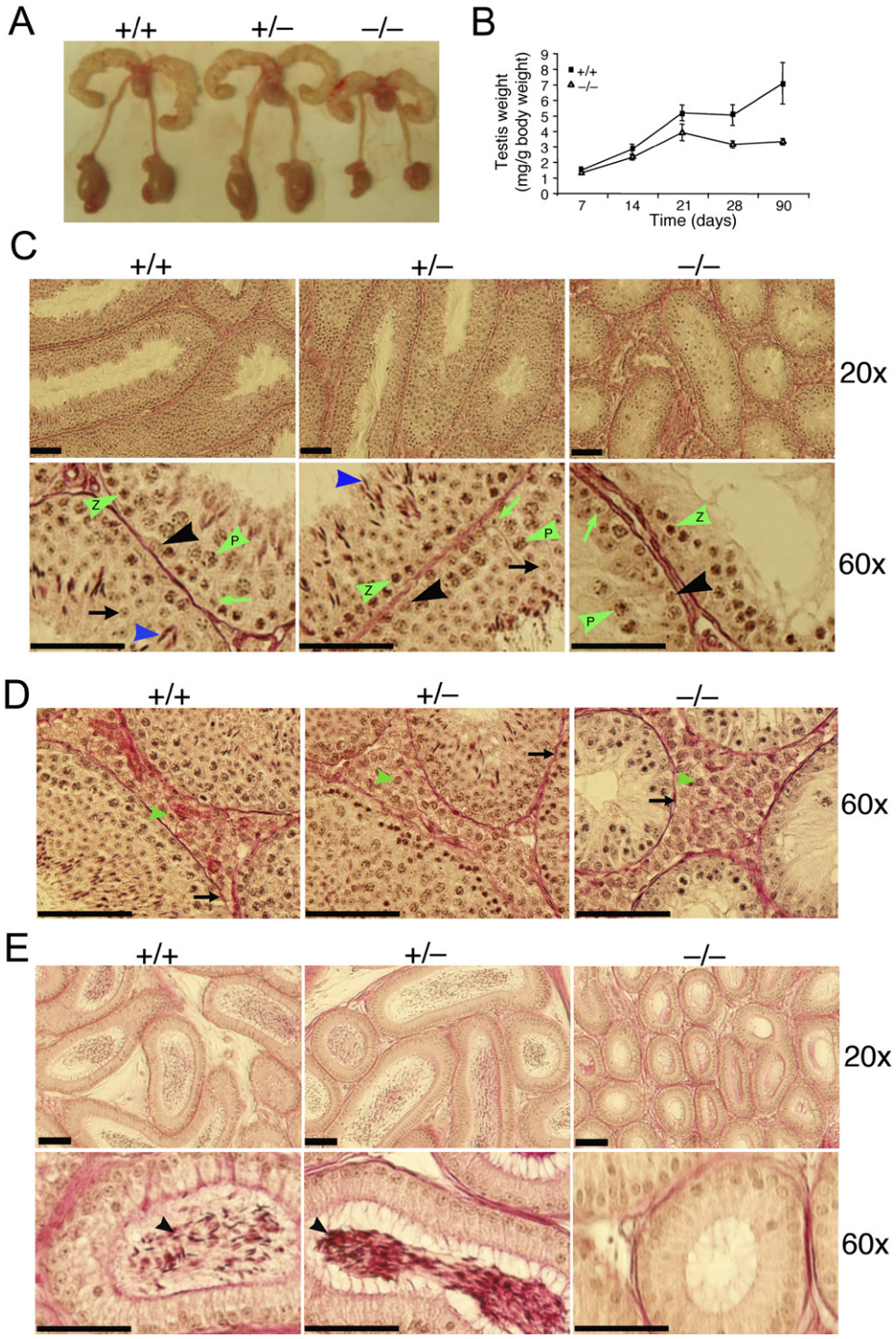

Figure 1. Impaired Spermatogenesis and Infertility of *Cyld*$^{-/-}$ Male Mice

(A) Reproductive organs of CYLD wild-type (+/+), heterozygous (+/–), and knockout (–/–) adult males (3 months).

(B) Testicular weight of *Cyld*$^{+/+}$ and *Cyld*$^{-/-}$ males at different ages, normalized to body weight. Data represent mean value of 20 mice for each time point with error bars indicating standard deviation.

(C) Histology of testicular tubules of *Cyld*$^{+/+}$, *Cyld*$^{+/-}$, and *Cyld*$^{-/-}$ adult males (3 months), presented at low (20×) and high (60×) magnifications. Black arrowheads, spermatogonia; green arrowheads with letter P, pachytene spermatocytes; green arrowheads with letter Z, zygotene spermatocytes; black arrows, round spermatids; blue arrowheads, elongating spermatids; green arrows, Sertoli cells.

(D) Histology to show comparable Leydig cells (green arrowheads) and lamina propria (black arrows) in the wild-type, heterozygous, and homozygous CYLD knockout mice.

physiological conditions remains enigmatic. Given the existence of a large number of DUBs (Nijman et al., 2005), it is likely that these enzymes may possess both redundant and essential biological functions in different tissues and cells.

In the present study, we demonstrate an unexpected and essential function of CYLD in the regulation of spermatogenesis and male fertility. The genetic deficiency of *Cyld* in mice attenuates the early wave of germ cell apoptosis and causes impaired spermatogenesis. This developmental defect is associated with constitutive activation of NF-κB and aberrant expression of antiapoptotic genes. Importantly, CYLD physically interacts with and inhibits the ubiquitination of receptor-interacting protein 1 (RIP1), a key upstream signaling molecule involved in the ubiquitin-dependent activation of IKK and NF-κB (Ea et al., 2006; Li et al., 2006; Wu et al., 2006). The loss of CYLD in testicular cells results in accumulation of ubiquitinated RIP1, which is associated with the chronic activation of IKK and NF-κB. These findings establish CYLD as a crucial DUB that regulates spermatogenesis and emphasize an essential role for CYLD in regulating RIP1 ubiquitination and NF-κB activation in testicular cells.

RESULTS

Impaired Spermatogenesis and Male Fertility in *Cyld*$^{-/-}$ Mice

To investigate the physiological functions of CYLD, we generated CYLD knockout mice (Reiley et al., 2006). Through the breeding process, we found that the homozygous CYLD knockout (*Cyld*$^{-/-}$) male mice were sterile, as they failed to produce offspring when mated with wild-type (*Cyld*$^{+/+}$) females. On the other hand, this sterility was not found with *Cyld*$^{-/-}$ females or heterozygous (*Cyld*$^{+/-}$) mice of both sexes. Consistent with these breeding results, the testis size of adult *Cyld*$^{-/-}$ males (12 wk old) was strikingly smaller than that of *Cyld*$^{+/+}$ and *Cyld*$^{+/-}$ littermates, while the other parts of the male reproductive organ appeared normal (Figure 1A and Figure S1, see the Supplemental Data available with this article online). The testicular atrophy in *Cyld*$^{-/-}$ mice was moderate during postnatal (PN) day 7–21 (prepubescent ages) but became drastic by PN28 (Figure 1B). This developmental defect was unlikely caused by hormones, since the seminal vesicle weight and the serum level of testosterone were comparable between the *Cyld*$^{+/+}$ and *Cyld*$^{-/-}$ mice (Figure S1 and data not shown). Further, the sterility and testicular atrophy were also detected in *Cyld*$^{-/-}$ mice bred to RAG1$^{-/-}$ background (data not shown). Since the *Cyld*$^{-/-}$*Rag1*$^{-/-}$ mice lacked lymphocytes, the sterile phenotype associated with *Cyld* deficiency was not caused by abnormal immune responses.

Histologic analyses of adult testes (12 wk old) revealed severe abnormalities in the seminiferous tubules of *Cyld*$^{-/-}$ mice, including reduction in both tubule cellularity and lumen size (Figure 1C, upper panels). Although spermatogonia and spermatocytes were readily found in the *Cyld*$^{-/-}$ seminiferous tubules (Figure 1C and Figure S2B), the postmeiotic germ cells (round and elongating spermatids) were scarce in the *Cyld*$^{-/-}$ tubules (Figure 1C, lower panels, black arrows and blue arrowheads). On the other hand, the *Cyld* deficiency did not seem to affect the Sertoli cells (Figure 1C, lower panels; Figure S2A). The abundance and morphology of Leydig cells were also comparable between the *Cyld*$^{-/-}$ and *Cyld*$^{+/+}$ testes (Figure 1D). Consistent with the spermatid deficiency in seminiferous tubles, the epididymides of *Cyld*$^{-/-}$ mice were devoid of spermatozoa (Figure 1E). The size of epididymis was also considerably reduced in the *Cyld*$^{-/-}$ mice. These findings clearly demonstrate an essential role for CYLD in regulating spermatogenesis and male fertility.

Cyld Deficiency Leads to Disorganization of Seminiferous Epithelium and Failure in Germ Cell Development

The stages of testis development are well defined in mice (McCarrey, 1993; Nebel et al., 1961). A few days postpartum, spermatogonial stem cells undergo mitotic divisions and initiate the process of spermatogenesis, leading to generation of spermatocytes around PN10. After meiosis, haploid spermatids appear around PN20 and then enter the final phase of differentiation to become spermatozoa around PN35. After this first wave of spermatogenesis, the cycle continues in adult mice with all stages of germ cells present in the seminiferous tubules. To identify the stage(s) of spermatogenesis affected by the *Cyld* deficiency, we analyzed the histology of testis sections prepared from mice of different ages. Prepubescent *Cyld*$^{-/-}$ mice (PN7 and PN14) did not show loss of germ cells in their seminiferous tubules (Figure 2A). The histology of PN21 tubules of *Cyld*$^{-/-}$ mice also did not show obvious degeneration. However, the *Cyld*$^{-/-}$ testes contained clustered pachytene spermatocytes in the center of some tubules, which appeared to have been sloughed off from Sertoli cells (Figure 2A, PN21). By PN28, the *Cyld*$^{-/-}$ mice displayed obvious defects in spermatogenesis, characterized by disorganization of seminiferous epithilium and abnormalities in spermatids (Figure 2A, PN28 and PN35). In addition to their reduced numbers, the spermatids displayed obvious signs of asynchronous and abnormal differentiation. The round spermatids lacked radial organization, and the elongating spermatids had incorrectly formed acrosomes. In contrast to these postmeiotic germ cells, spermatogonia and early spermatocytes were either normal or more abundant in the different stages of *Cyld*$^{-/-}$ seminiferous tubules (Figure 2A and Figure S2B). Thus, the loss of CYLD causes disorganized seminiferous epithelium and impaired germ cell development.

(E) Histology of epididymis of *Cyld*$^{+/+}$ and *Cyld*$^{-/-}$ adult males showing the smaller size and lack of sperm (black arrowheads) in the epididymis of *Cyld*$^{-/-}$ mice.
Bars in (C–E) = 400 μm.

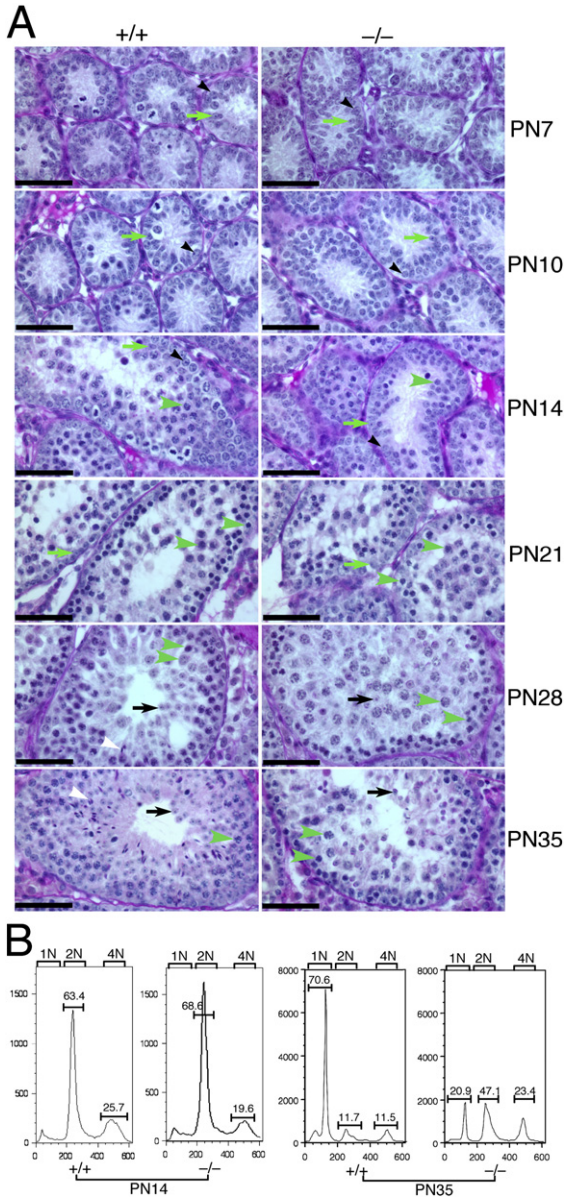

Figure 2. Progressive Defect in Testis Development of *Cyld*$^{-/-}$ Mice

(A) Histology of developing testes from *Cyld*$^{+/+}$ and *Cyld*$^{-/-}$ males presented as 40× magnifications. Representative spermatogonia (black arrowheads), spermatocytes (green arrowheads), round spermatids (black arrows), elongating spermatids (while arrowheads), and Sertoli cells (green arrows) are indicated. Bars = 400 μm.

(B) Germ cells of *Cyld*$^{+/+}$ and *Cyld*$^{-/-}$ mice (PN14 and PN35) were stained with propidium iodide and analyzed by flow cytometry (using FACScan; Becton-Dickinson) on the basis of DNA content and nuclear size. Fifty thousand cells or events were analyzed for each sample, and the histograms were generated using the Modfit LT program (Verity Software House, Inc.) with the percentages of the cell populations indicated. The 4N peak represents cells that are either at the S phase of mitotic division or primary spermatocytes at prophase I of the meiotic division, with the latter being predominant (Malkov et al., 1998). The 2N peak is composed of spermatogonia, preleptotene spermatocytes, and secondary spermatocytes between the two meiotic divisions (Malkov et al., 1998). The 1N peak is composed of round and elongating spermatids.

Using flow cytometry technique (Malkov et al., 1998), we further examined the stages of spermatogenesis affected by the *Cyld* deficiency. As expected, the testes of prepubescent wild-type mice (PN14) contained predominantly 2N cells and a small population of 4N cells (Figure 2B, +/+ PN14). The 2N population includes spermatogonia and primary spermatocytes, whereas the 4N population contains meiotic spermatocytes as well as S phase spermatogonia (Malkov et al., 1998). The testes of wild-type PN35 mice had an abundant population of 1N cells, representing postmeiotic (haploid) round and elongating spermatids, as well as small populations of 2N and 4N cells (Figure 2B, +/+ PN35). Consistent with the histologic data, the prepubescent *Cyld*$^{-/-}$ mice did not show obvious germ cell deficiencies, and these mutant animals even had a slight increase in the proportion of 2N testicular cells (Figure 2B, −/− PN14). In contrast, the testes of PN35 *Cyld*$^{-/-}$ males had a drastic reduction in the proportion of 1N spermatids and a relative increase in the proportion of 2N and 4N cells (Figure 2B, −/− PN35). These results are similar to those observed with mice lacking proapoptotic proteins, Bax or Bim and Bik (Coultas et al., 2005; Knudson et al., 1995; Russell et al., 2002). Together, these results suggest that the *Cyld* deficiency attenuates the generation of postmeiotic germ cells during spermatogenesis.

CYLD Is Dispensable for Germ Cell Proliferation but Is Critical for Regulating Germ Cell Apoptosis

To elucidate the mechanism by which CYLD regulates spermatogenesis, we examined whether the loss of CYLD affected the proliferation or survival of germ cells. Immunohistochemistry (IHC) of proliferating cell nuclear antigen (PCNA) revealed robust proliferation of testicular cells, predominantly spermatogonia and primary spermatocytes, in different ages of wild-type mice (Figure S3). Moreover, the testes of age-matched *Cyld*$^{-/-}$ mice displayed similar levels of PCNA staining at different stages of spermatogenesis. Similar results were obtained using bromodeoxyuridine incorporation assays (data not shown). Thus, loss of CYLD does not affect the proliferation of germ cells.

We next analyzed germ cell apoptosis by TUNEL assay, which is based on nuclear DNA fragmentation (Gavrieli et al., 1992). Prior studies demonstrate that the first wave of spermatogenesis is associated with extensive germ cell apoptosis (Mori et al., 1997; Print and Loveland, 2000; Rodriguez et al., 1997). Consistently, we detected apoptotic cells in the testicular tubules of wild-type mice ranging from PN7 to PN35 (Figure 3A, +/+). The apoptotic cells included both spermatogonia and spermatocytes, judging from their morphology and tubular localization (Figure 3C). Interestingly, the early phase apoptosis (PN7 and PN14) was markedly attenuated in the *Cyld*$^{-/-}$ testes (Figure 3A, −/−). This finding was not due to tubular variations, as confirmed by quantification of apoptotic cells from 50 randomly selected tubules on four different slides (Figure 3B). Moreover, apoptotic cells were detected in the *Cyld*$^{-/-}$ testes at the stage of PN21 (Figures 3A and 3B), which became remarkably more abundant at the

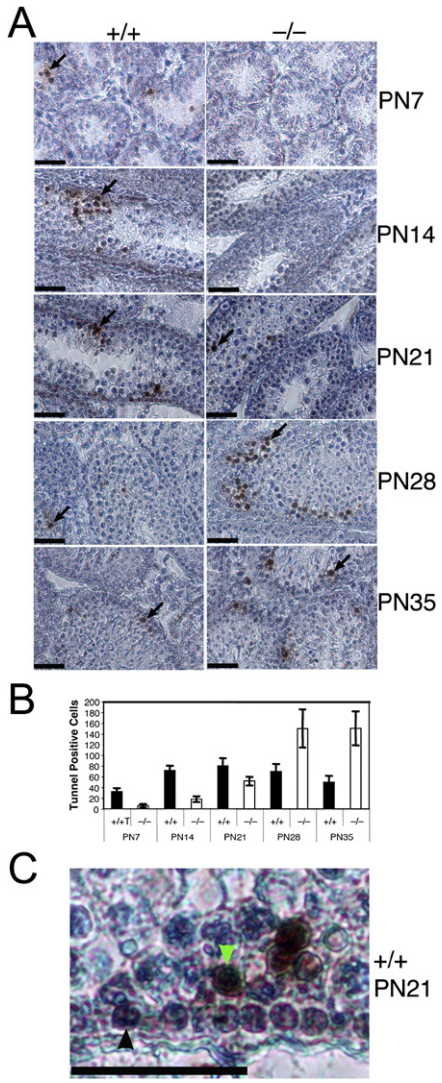

Figure 3. Deregulated Apoptosis in *Cyld*$^{-/-}$ Testicular Cells

(A) Germ cell apoptosis in different stages of testes. Testis sections from *Cyld*$^{+/+}$ and CYLD knockout (–/–) mice were subjected to TUNEL assay. Representative apoptotic cells are indicated by arrows. Magnification, 30×; bars = 400 μm.

(B) The apoptotic cells in (A) were counted in 50 random seminiferous tubules of four different sections and presented as mean value with error bars indicating standard deviation. The p values of t tests are < 0.0001, < 0.0001, 0.0024, 0.0058, and 0.001 for PN7, PN14, PN21, PN28, and PN35, respectively.

(C) Higher magnification of PN21 wild-type testis section, showing an apoptotic spermatogonium (black arrowhead) and apoptotic spermatocyte (green arrowhead). Magnification, 100×; bars = 400 μm.

late stages of the spermatogenesis (Figures 3A and 3B, PN28 and PN35). In fact, at these stages, the level of apoptosis in *Cyld*$^{-/-}$ testes was much higher compared to the *Cyld*$^{+/+}$ testes. Similar results were obtained when Cleaved Caspase-3 level was used as an indicator of apoptosis (Figure S4). Thus, the loss of CYLD attenuates testicular apoptosis at early stages of spermatogenesis, resulting in heightened apoptosis and testicular degeneration at late PN stages. These results are consistent with the finding that the *Cyld*$^{-/-}$ testes contain more early phase germ cells but display tubular degeneration at late stages of spermatogenesis (Figure 2). Of note, the early wave of germ cell apoptosis is essential for spermatogenesis, since it may function to maintain a proper balance between germ cells and Sertoli cells (Mori et al., 1997; Print and Loveland, 2000; Rodriguez et al., 1997). Defect in early wave apoptosis is believed to promote testicular cell death and tubule degeneration at later PN stages (Coultas et al., 2005; Print et al., 1998).

Aberrant Expression of Apoptosis Inhibitors in *Cyld*$^{-/-}$ Testicular Cells

The Bcl-2 family of proteins plays a crucial role in regulating germ cell apoptosis and spermatogenesis (Print and Loveland, 2000). Impaired early wave germ cell apoptosis and late-stage spermatogenesis have been observed in mice with transgenic expression of Bcl-2 or Bcl-XL and germ-line inactivation of pro-apoptotic Bcl-2 members (Coultas et al., 2005; Furuchi et al., 1996; Print et al., 1998; Rodriguez et al., 1997; Russell et al., 2002). Because of the similar phenotype between *Cyld*$^{-/-}$ mice and Bcl-2 family transgenic mice, we examined the effect of *Cyld* deficiency on the expression of Bcl-2 family members. A low level of Bcl-2 protein was detected in the testes of PN14 wild-type mice (Figure 4A). However, a substantially higher level of Bcl-2 was detected in the age-matched *Cyld*$^{-/-}$ testes (Figure 4A). In contrast, the expression levels of two proapoptotic Bcl-2 members, Bax and Bim, in *Cyld*$^{-/-}$ testes were either comparable to or slightly lower than those of wild-type testes. Overexpression of Bcl-2 was also detected in the later stages of *Cyld*$^{-/-}$ testes (Figure 4B). Moreover, the aberrant expression of Bcl-2 in *Cyld*$^{-/-}$ germ cells was further confirmed by IHC in PN14 testes, which showed heightened Bcl-2 expression predominantly in the spermatogonia and spermatocytes of *Cyld*$^{-/-}$ seminiferous tubules (Figure 4C). Thus, as seen with the Bcl-2 transgenic studies (Rodriguez et al., 1997), Bcl-2 overexpression occurs at different PN stages of *Cyld*$^{-/-}$ testes but selectively affects the early wave of germ cell apoptosis. Real-time PCR assays revealed that the loss of CYLD also caused overexpression of several other antiapoptotic genes, including Bcl-XL, c-IAP1, and c-IAP2, in different stages of testicular cells (Figure 4D and data not shown). These results provide mechanistic insight into the attenuation of early wave of apoptosis in *Cyld*$^{-/-}$ testes. Of note, the expression of IκBα was also upregulated in the *Cyld*$^{-/-}$ testes (Figure 4D). Since expression of IκBα as well as the antiapoptotic genes is under the control of transcription factor NF-κB (Catz and Johnson, 2001; Karin and Lin, 2002), these findings suggest the possible involvement of abnormal NF-κB activation in *Cyld*$^{-/-}$ testicular cells.

Cyld Deficiency Results in Constitutive Activation of NF-κB in Testes

NF-κB is normally sequestered in the cytoplasm by association with an inhibitory protein, IκBα. Activation of NF-κB

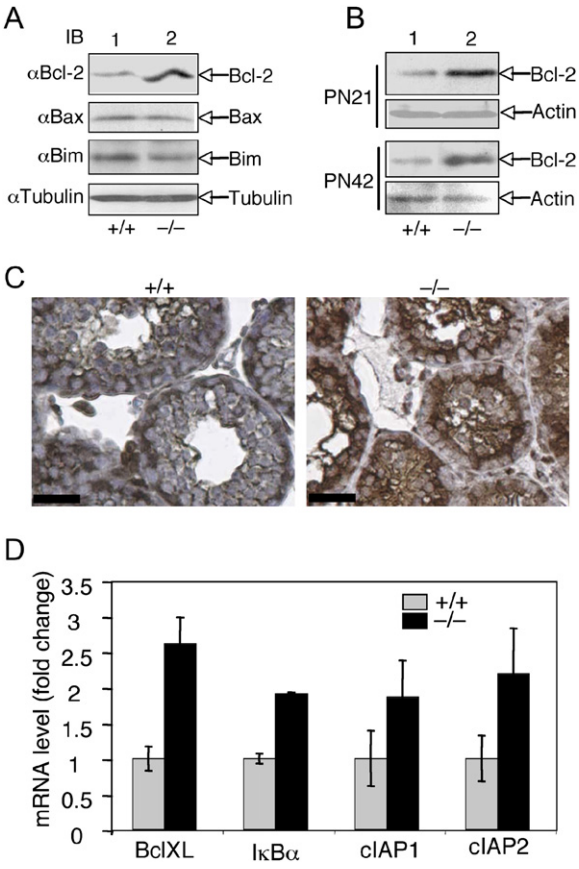

Figure 4. Aberrant Expression of Antiapoptotic Genes in *Cyld*$^{-/-}$ Testicular Cells

(A) Whole-cell lysates were prepared from the germ cells of *Cyld*$^{+/+}$ and *Cyld*$^{-/-}$ males at PN14 and subject to IB assays to detect the expression of the indicated proteins.

(B) IB of Bcl2 and actin in testicular cells at PN21 and PN42.

(C) Testis sections were prepared from *Cyld*$^{+/+}$ and *Cyld*$^{-/-}$ males at PN14 and subjected to IHC with anti-Bcl-2 antibody. Bcl-2-positive cells are stained brown. Magnification, 30×; bars = 400 μm.

(D) RT-PCR was performed using RNA isolated from PN14 germ cells to measure the mRNA level of the indicated genes. Data represent mean values of three independent experiments with error bars indicating standard deviation.

by various cellular stimuli involves stimulation of the IKK complex, which is composed of two catalytic subunits (IKKα and IKKβ) and a regulatory subunit (IKKγ). Upon activation, IKK phosphorylates IκBα, triggering its degradation and nuclear translocation of active NF-κB. Within the nucleus, NF-κB transactivates various target genes, including those encoding antiapoptotic proteins and IκBα. To examine NF-κB signaling, we first analyzed in vivo phosphorylation of IκBα by IHC (Figure 5). The wild-type testes contained a low number of cells with phosphorylated IκBα (Figure 5, +/+). Remarkably, however, a much larger number of cells were stained positive for phosphorylated IκBα in the *Cyld*$^{-/-}$ testes (Figure 5, −/−). Consistent with the Bcl-2 induction, the increased IκBα phosphorylation was seen in *Cyld*$^{-/-}$ testes at all stages of development. Based on their morphology, these cells appeared to include predominantly spermatogonia (Figure 5, black arrowheads). Spermatocytes were also stained positive, albeit with lower intensity (green arrowheads). Compared to negative control, some Sertoli cells appeared to also have weak staining of phosho-IκBα. However, since such staining was very weak, it might be due to the detection of unphosphorylated IκBα. In general, no strong phospho-IκBα was detected in Sertoli cells (Figure 5, black arrows). This result suggested that loss of CYLD causes constitutive activation of the NF-κB signaling pathway in testicular germ cells.

To further examine the activation of NF-κB in *Cyld*$^{-/-}$ testicular cells, we performed electrophoresis mobility shift assays (EMSA) to detect the DNA binding activity of nuclear NF-κB. Consistent with the IκBα phosphorylation data, the germ cells of *Cyld*$^{+/+}$ and *Cyld*$^{+/-}$ mice had a low basal level of nuclear NF-κB DNA-binding activity (Figure 6A, lanes 1 and 2). In contrast, the cells derived from *Cyld*$^{-/-}$ mice displayed a strikingly higher level of NF-κB activity (Figure 6A, lane 3). This difference was not due to loading variation as demonstrated by the equal DNA-binding activity of a constitutive nuclear factor, NF-Y (Figure 6A, lanes 4-6). Moreover, the specificity of the NF-κB DNA binding was confirmed by supershift assays using antibodies for two major NF-κB members, p50 and p65 (Figure 6B), and by probe competition assays (Figure 6C). The hyperactivation of NF-κB was detected in different stages of *Cyld*$^{-/-}$ testicular cells (Figure 6A and Figure S5A).

Consistent with the activation of NF-κB, the steady-state level of IκBα protein was significantly reduced in *Cyld*$^{-/-}$ testes (Figure 6D). This result was not due to reduced IκBα gene expression, since the IκBα mRNA was even upregulated in *Cyld*$^{-/-}$ testes (Figure 4D), supporting the previous finding that IκBα gene expression is under the control of NF-κB (Sun et al., 1993). Taken together with the hyperphosphorylation of IκBα (Figure 5), these findings suggested that the *Cyld* deficiency caused spontaneous activation of the IKK. This prediction was confirmed by a parallel kinase assay, which showed hyperactivation of IKK in different stages of *Cyld*$^{-/-}$ testes (Figure 6E). Thus, during spermatogenesis, CYLD is essential for the control of signaling events involved in the activation of IKK and its target transcription factor NF-κB.

Essential Role for CYLD in Controlling RIP1 Ubiquitination in Testicular Cells

IKK activation by cytokines and mitogens appears to involve K63-linked ubiquitination of IKKγ, as well as upstream signaling molecules (Chen, 2005). To further elucidate the molecular mechanism by which CYLD regulates IKK and NF-κB, we examined whether the loss of CYLD resulted in aberrant ubiquitination of signaling factors. Although we were unable to detect significant ubiquitination of IKKγ and another signaling factor, TRAF6, in the *Cyld*$^{-/-}$ testicular cells (Figure 7A and data not shown), we found that these mutant germ cells had a marked accumulation of polyubiquitinated RIP1 at different PN stages (Figure 7A, lanes 2 and 4, data not shown). Of

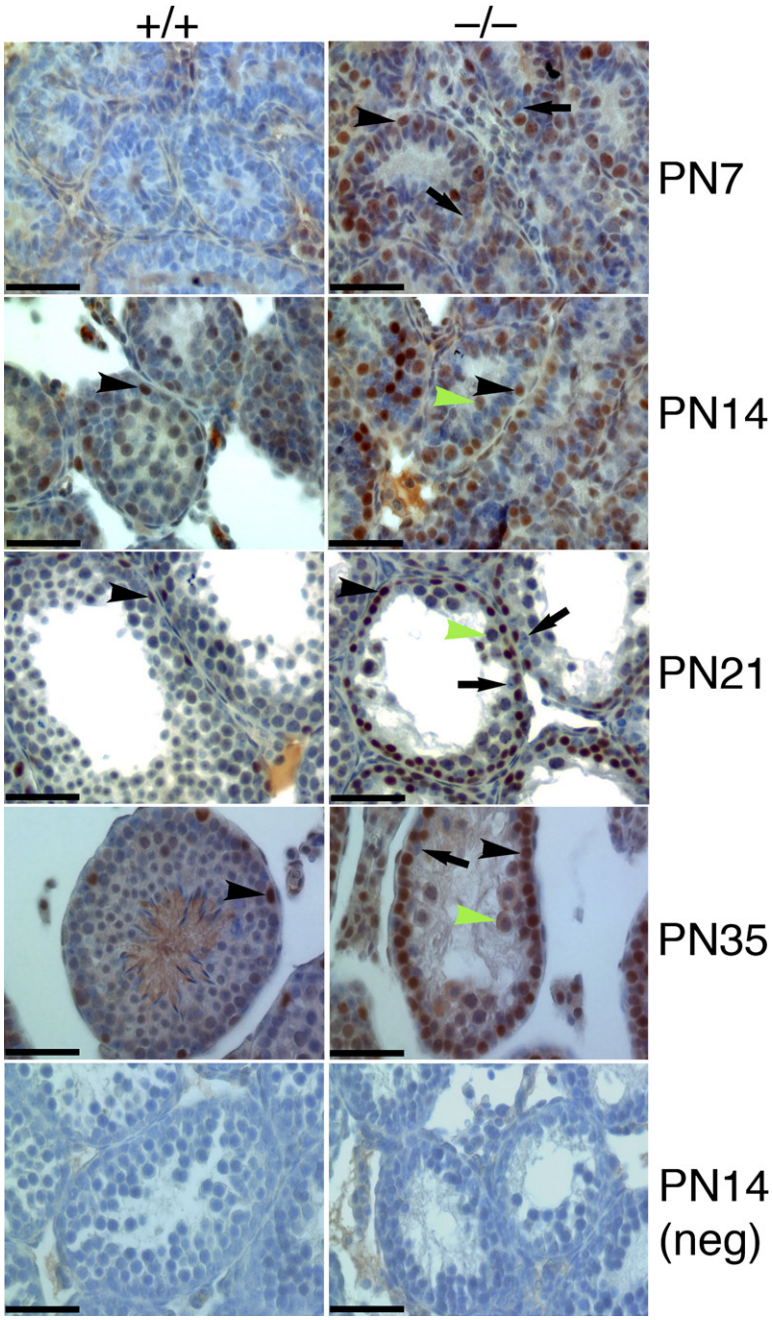

Figure 5. Constitutive Phosphorylation of IκBα in *Cyld*$^{-/-}$ Germ Cells

Testis sections from the indicated ages of mice were subjected to IHC using a phospho-specific anti-IκBα antibody. Magnification, 40×; bars = 400 μm. Black arrowheads, green arrowheads, and black arrows indicate spermatogonia, spermatocytes, and Sertoli cells, respectively.

note, RIP1 ubiquitination is known as a critical step in cytokine-induced activation of IKK (Ea et al., 2006; Li et al., 2006; Wu et al., 2006). Although the stimulus that triggers NF-κB signaling in testicular cells is unclear, the accumulation of RIP1 in *Cyld*$^{-/-}$ cells suggests that CYLD plays an essential role in negatively regulating RIP1 ubiquitination and signaling function in testicular cells.

We further assessed the role of CYLD in inhibiting RIP1 ubiquitination and signaling using a transfection model. As previously reported (Li et al., 2006), overexpressed RIP1 underwent constitutive polyubiquitination (Figure S6A), which was consistent with its ability to induce NF-κB activation (Figure S6B). Importantly, both RIP1 ubiquitination and RIP1-induced NF-κB activation were inhibited by wild-type (Wt) CYLD but not a catalytically inactive CYLD mutant (Mut) (Reiley et al., 2006) (Figures S6A and S6B). To further elucidate the role of CYLD in regulating the inducible ubiquitination of RIP1, we analyzed the ubiquitination of endogenous RIP1 induced by TNF-α in HeLa cells. Consistent with prior studies (Ea et al., 2006), at the early point of TNF-α stimulation, RIP1 is predominantly conjugated with K63-linked ubiquitin chains (Figure S6C). Moreover, the inducible ubiquitination of RIP1 was blocked by CYLD (Figure S6D).

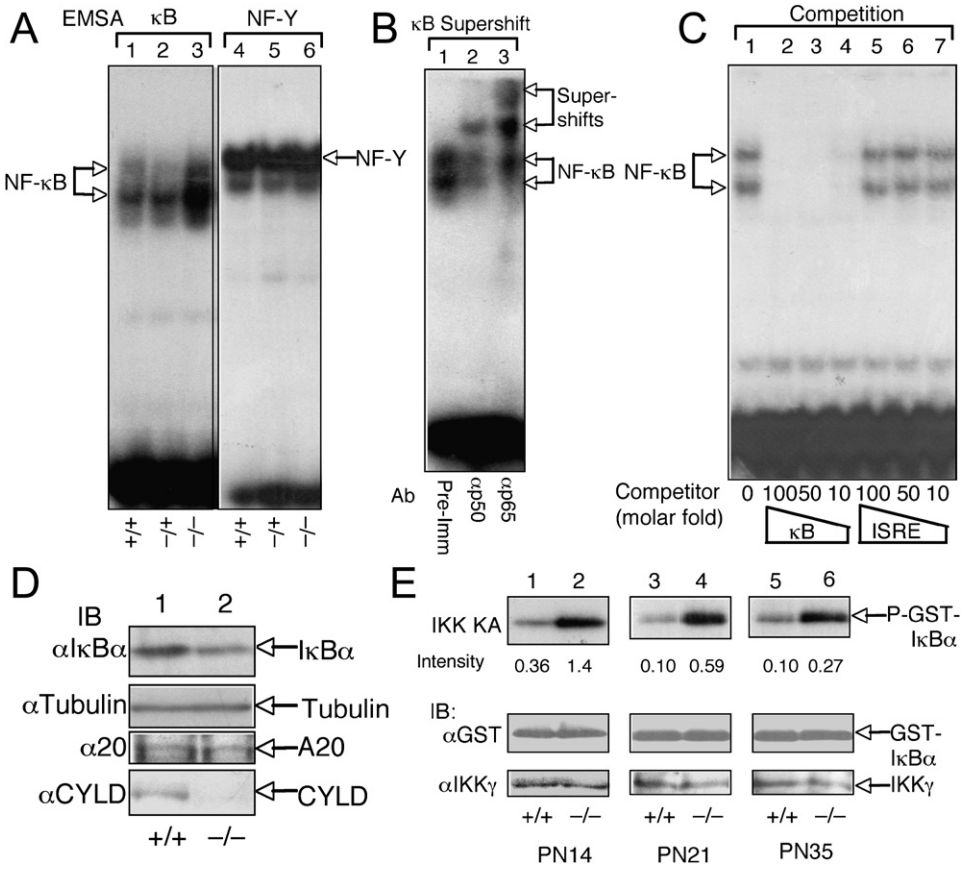

Figure 6. *Cyld* Deficiency Results in Constitutive Activation of NF-κB and IKK in Testicular Cells

(A) Nuclear extracts were prepared from $Cyld^{+/+}$, $Cyld^{+/-}$, and $Cyld^{-/-}$ males at PN14 and subjected to EMSA using ^{32}P-radiolated probes for NF-κB or the constitutive transcription factor NF-Y.

(B) EMSA was performed using the $Cyld^{-/-}$ nuclear extract in the presence of either a preimmune serum or antibodies to two major NF-κB subunits.

(C) EMSA was performed using the $Cyld^{-/-}$ nuclear extract in the presence of increasing doses of the κB probe or an unrelated probe (interferon-stimulated response element, ISRE).

(D) IB was performed using whole-cell lysates of PN14 testes to show reduced level of IκBα in $Cyld^{-/-}$ germ cells.

(E) IKK complex was isolated by IP (using anti-IKKγ) from whole-cell lysates of different stages of germ cells and subjected to in vitro kinase assays using GST-IκBα(1-54) as substrate. The intracellular levels of IKKγ were monitored by IB.

CYLD Physically Associates with RIP1

The potent activity of CYLD in suppressing RIP1 ubiquitination under both transfected and endogenous conditions suggests the intriguing possibility that RIP1 may be a target of CYLD. We further addressed this possibility by analyzing the CYLD-RIP1 physical interaction under endogenous conditions in $Cyld^{+/+}$ testicular cells. Indeed, CYLD and RIP1 were present in a stable complex, which was coprecipitated by the anti-CYLD antibody (Figure 7B, lane 2) or anti-RIP1 antibody (Figure S5B). This binding was specific, since RIP1 was not pulled down by a preimmune serum (Figure 7B, lane 1). The CYLD-RIP1 physical interaction was also readily detected when they were coexpressed in 293T cells (Figure 7C). Taken together with CYLD's role in suppressing RIP1 ubiquitination, these results establish RIP1 as a physiological target of CYLD in testicular cells.

Loss of CYLD Causes Constitutive Association of RIP1 with IKK in Testicular Cells

A crucial mechanism of IKK activation by RIP1 involves binding of ubiquitinated RIP1 by the IKK regulatory subunit, IKKγ (Ea et al., 2006; Wu et al., 2006). Since the constitutive ubiquitination of RIP1 in $Cyld^{-/-}$ testicular cells was associated with IKK activation, we examined whether the *Cyld* deficiency caused constitutive association of IKKγ with RIP1. Only a small amount of IKKγ was coprecipitated with RIP1 from the $Cyld^{+/+}$ and $Cyld^{+/-}$ testicular cells (Figure 7D, lanes 1 and 2). In sharp contrast, a large amount of IKKγ was coprecipitated with RIP1 from the $Cyld^{-/-}$ cells (Figure 7D, lane 3). This result was not due to the upregulation of RIP1 and IKKγ expression (Figure 7D, middle and bottom panels). Together, these results suggest that loss of CYLD results in uncontrolled ubiquitination of RIP1, which in turn recruits and activates

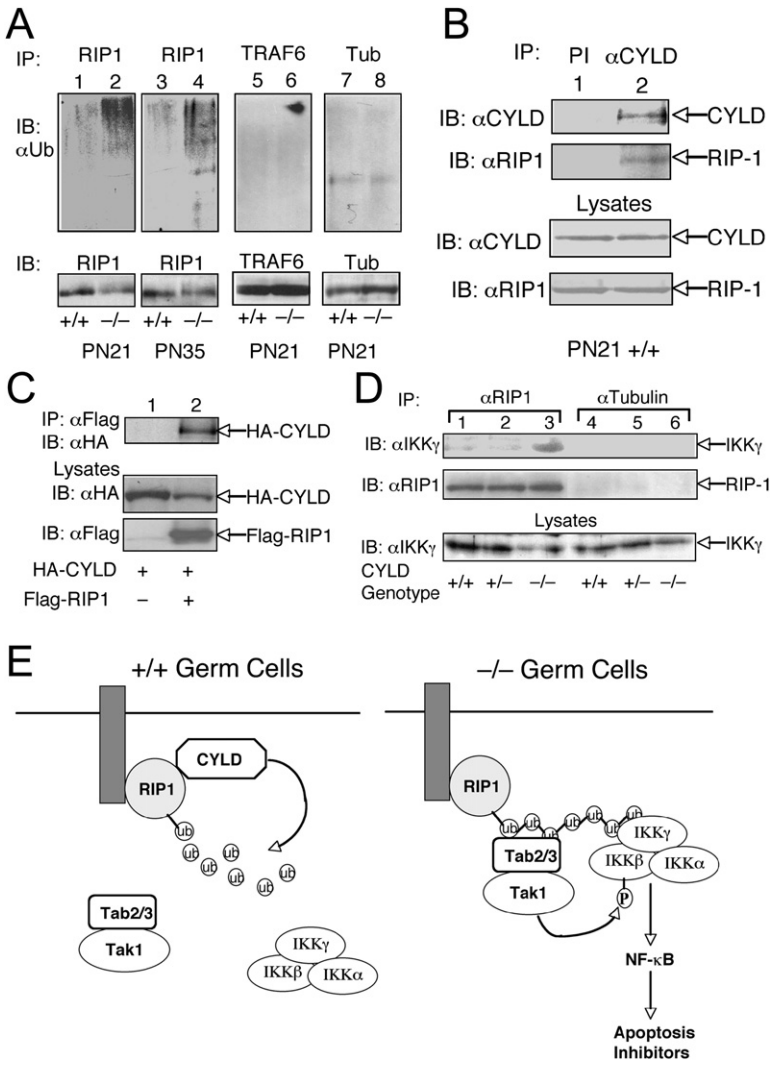

Figure 7. RIP1 Is a Target of *Cyld*$^{-/-}$ in Testicular Cells

(A) Accumulation of ubiquitinated RIP1 in *Cyld*$^{-/-}$ testicular cells. Whole-cell lysates were prepared from the indicated ages of *Cyld*$^{+/+}$ or *Cyld*$^{-/-}$ males. RIP1 was isolated by IP followed IB using anti-ubiquitin to detect ubiquitinated RIP1.

(B) Physical interaction of endogenous CYLD and RIP1. Whole-cell lysates were isolated from *Cyld*$^{+/+}$ germ cells (PN21) and subjected to IP using either a control preimmune serum or anti-CYLD. The immune complexes were subjected to IB to detect the coprecipitated RIP1 and CYLD (panels 1 and 2). Cell lysates were also subjected to direct IB to monitor the expression levels of CYLD and RIP1 (panels 3 and 4).

(C) Physical interaction of transfected CYLD and RIP1. 293T cells were transfected with HA-CYLD either in the absence (−) or presence (+) of Flag-RIP1. The RIP1 complex was isolated by IP using anti-Flag, and the coprecipitated CYLD was detected by IB using anti-HA (panel 1). Cell lysates were also subjected to direct IB to monitor the expression levels of CYLD and RIP1 (panels 2 and 3).

(D) *Cyld* deficiency results in RIP1/IKK association. Whole-cell lysates from *Cyld*$^{+/+}$, *Cyld*$^{+/-}$, and *Cyld*$^{-/-}$ PN21 germ cells were subject to IP using either anti-RIP1 or anti-tubulin, and the immune complexes were analyzed by IB to detect IKKγ and RIP1 (top two panels). Expression level of IKKγ was analyzed by direct IB (bottom panel).

(E) Model of CYLD signaling function in early germ cells. Early germ cells (predominantly spermatogonia) are likely exposed to an NF-κB stimulus, resulting in RIP1 ubiquitination. Under normal conditions, the ubiquitinated RIP1 is rapidly deubiquitinated by CYLD, thus preventing productive activation of NF-κB and facilitating the early wave of germ cell apoptosis. *Cyld* deficiency causes accumulation of ubiquitinated RIP1, leading to ubiquitin-dependent recruitment IKK complex as well as IKK-activating kinases (e.g., Tak1). The uncontrolled NF-κB signaling in turn results in aberrant expression of apoptosis inhibitory genes and the attenuation of germ cell apoptosis.

IKK, leading to deregulated NF-κB activation and aberrant expression of its target genes.

DISCUSSION

This study demonstrates an essential role for CYLD in regulating spermatogenesis and male fertility. CYLD functions by negatively regulating NF-κB activation, thereby preventing abnormal expression of apoptosis inhibitors. The effect of *Cyld* deficiency on spermatogenesis appears to be progressive. As early as PN7, the *Cyld*$^{-/-}$ testicular cells display heightened phosphorylation of IκBα, indicating NF-κB activation. Severe attenuation of germ cell apoptosis can be detected between PN7 and PN14, which is associated with upregulation of Bcl-2 and Bcl-XL, as well as other antiapoptotic genes. The prepuberal *Cyld*$^{-/-}$ mice show abnormally developed seminiferous lumens and gross disorganization of the seminiferous epithelium. Eventually, spermatogenesis collapses in adult *Cyld*$^{-/-}$ animals, with only Sertoli cells, spermatogonia, and early stage spermatocytes remaining in the seminiferous tubules.

The defect of *Cyld*$^{-/-}$ mice in spermatogenesis is similar, although not identical, to that of mice lacking the Bcl2 family of proapoptotic members or transgenically expressing Bcl-2 family of antiapoptotic members in spermatogonia (Coultas et al., 2005; Furuchi et al., 1996; Print et al., 1998; Rodriguez et al., 1997; Russell et al., 2002). Germ-line inactivation of the proapoptotic gene Bax, or combined inactivation of the proapoptotic genes Bim and Bik, results in the block of early wave of apoptosis and impaired late stage of spermatogenesis (Coultas et al., 2005; Knudson et al., 1995; Russell et al., 2002). Similarly, transgenic expression of the antiapoptotic factors, Bcl-2 or Bcl-XL, in male germ cells impairs spermatogenesis (Furuchi et al., 1996; Rodriguez et al., 1997). It is

generally thought that impaired early wave of germ cell apoptosis increases the ratio of developing germ cells to the postmitotic Sertoli cells, which compromises the ability of Sertoli cells to maintain the specialized multicompartment environment required for spermatogenesis in adults. Our finding that *Cyld* deficiency causes aberrant expression of Bcl-2 and Bcl-XL provides a molecular insight into the mechanism by which CYLD regulates spermatogenesis. Of course, it is possible that the spermatogenic defect in $Cyld^{-/-}$ mice may also involve additional mechanisms, such as deregulated signaling or cell cycle events in spermatogonia and early spermatocytes.

We have obtained genetic evidence that establishes CYLD as an essential negative regulator of NF-κB signaling in testes. Our data indicate that the early phase germ cells may be constantly exposed to NF-κB stimuli, but the magnitude of NF-κB activation is subjected to tight control by negative regulators, including CYLD. Indeed, the loss of CYLD is sufficient for triggering heightened NF-κB signaling, as revealed by activation of its upstream kinase IKK, IκBα phosphorylation, and nuclear DNA-binding activity of NF-κB members. The deregulated NF-κB signaling occurs predominantly in spermatogonia and spermatocytes. Since NF-κB is a potent inducer of Bcl-2 and Bcl-XL as well as other prosurvival genes (Catz and Johnson, 2001; Feuillard et al., 2000; Karin and Lin, 2002), the chronic activation of NF-κB in $Cyld^{-/-}$ testicular cells likely contributes to the attenuated germ cell apoptosis during the early wave of spermatogenesis.

Although CYLD is a DUB clearly involved in signal transduction, how CYLD regulates protein ubiquitination in different physiological processes remains unclear. Since the number of ubiquitinated proteins is far larger than that of DUBs (Nijman et al., 2005), it is likely that each DUB may mediate the deubiquitination of a group of proteins. On the other hand, due to the potential functional redundancy among the DUBs and variation in accessory factors, the essential role of DUBs may vary in different cell systems. As depicted in Figure 7E, we have obtained biochemical and genetic evidence that demonstrates RIP1 as a major target of CYLD in testicular cells. On the other hand, the loss of CYLD did not affect the ubiquitination or expression of two other candidate molecules, TRAF2 and TRAF6 (Figure 7A, Figure S7, and data not shown). K63-linked ubiquitination of RIP1 is known to create a platform for recruiting IKK as well as its activating kinase Tak1 (Ea et al., 2006; Li et al., 2006; Wu et al., 2006). We have shown that at least in HeLa cells, the TNF-α-stimulated K63-ubiquitination of RIP1 is inhibited by CYLD. In testicular cells, CYLD forms a complex with RIP1 and inhibits RIP1 ubiquitination. Thus, an attractive model is that RIP1 undergoes ubiquitination in early phase germ cells (mostly spermatogonia) probably due to the exposure of these cells to certain chronic stimuli. However, the ubiquitinated RIP1 is normally deubiquitinated by CYLD, thus preventing hyperactivation of NF-κB signaling. The *Cyld* deficiency results in accumulation of ubiquitinated RIP1, leading to ubiquitin-dependent recruitment of IKK complex and its upstream kinases (e.g., Tak1) (Figure 7E). Indeed, we have shown that IKK is constitutively associated with RIP1 and activated in the $Cyld^{-/-}$ testicular cells. It is currently unclear what environmental signals stimulate the ubiquitination of RIP1 in germ cells. Prior studies suggest that TNF-α induces germ cell survival, which appears to involve NF-κB (Suominen et al., 2004). Since TNF-α induces K63 ubiquitination of RIP1 in other cell systems, it is tempting to speculate that TNF-α may play a role in the induction of RIP1 ubiquitination and NF-κB activation in germ cells. However, the involvement of other germ cell stimuli is also highly possible because TNF receptor is primarily expressed on somatic cells in the testes (De et al., 1993).

Our findings provide an example for how deregulated protein ubiquitination and NF-κB activation affect a developmental process. The identification of CYLD as an essential regulator of spermatogenesis also raises a number of questions. For example, is the requirement of CYLD in spermatogenesis germ cell intrinsic? Is CYLD required only for the first wave of spermatogenesis? Is the spermatogenic defect of $Cyld^{-/-}$ mice solely due to attenuated germ cell apoptosis or also involving other molecular abnormalities? Regarding the DUB function of CYLD, it remains unclear whether RIP1 is the only target of CYLD involved in spermatogenesis and whether RIP1 undergoes K63-linked ubiquitination in testicular germ cells. Notwithstanding, our findings establish CYLD as a crucial regulator of spermatogenesis and shed light on the mechanism of its function in this important biological process.

EXPERIMENTAL PROCEDURES

Mice

Cyld knockout mice (in C57BL6/DBA mixed genetic background) were generated as described (Reiley et al., 2006). $Cyld^{+/-}$ mice were intercrossed to generate $Cyld^{-/-}$ and $Cyld^{+/+}$ littermates. Genotyping and housing were as described (Reiley et al., 2007). Animal experiments were performed in accordance with protocols approved by the Pennsylvania State University College of Medicine Institutional Animal Care and Use Committee.

Cell Lines and Transfection

Human embryonic kidney cell line 293T (provided by Dr. Barbara Miller) and HeLa cells were cultured in DMEM media. The cells were seeded in 6-well plates and transfected using Lipofectamine-2000 (Invitrogen).

Plasmids, Antibodies, and Reagents

pcDNA-HA-CYLD, pcDNA-HA-CYLD(1–932) (lacking DUB activity), pcDNA-HA-ubiquitin, and pGex-IκBα(1-55) were described previously (Reiley et al., 2005, 2006). HA-ubiquitin K48 and HA-ubiquitin K63 were provided by Dr. Zhijian Chen (Ea et al., 2006). Flag-tagged RIP1 was provided by Margaret K. Offermann (Kaiser and Offermann, 2005). Antibodies for Bcl-2, Bim, Bax, Cleaved Caspase-3 (Asp175), and phospho-IκBα (Ser32/36) were from Cell Signaling. Anti-GATA1 (N6), anti-IKKα (H470), anti-IKKγ (FL-419), anti-PCNA (FL-261), and anti-Tubulin (TU-02) were from Santa Cruz. Anti-flag (D-8), anti-HA-HRP (3F10), and anti-RIP1 were from Sigma, Roche, and BD Biosciences, respectively. Anti-SCP3 (ab15092) was from Abcam Inc. Anti-ubiquitin was provided by Dr. Vincent Chau. Other antibodies have been described previously (Reiley et al., 2004, 2005).

Histology and IHC

Testes and epididymides were removed from sacrificed mice and immersed in 10 volumes of ice-cold neutral buffered formalin or Bouins

fluid at 4°C for 24 hr. Following dehydration, the tissues were embedded in paraffin, sectioned, and stained with periodic acid Schiff reagent and counter stained with hematoxylin. Pictures were taken from typical sections.

For IHC analysis, Bouins-fixed, paraffin-embedded testicular sections were deparaffinized, hydrated by a successive series of ethanol, rinsed in dH_20, and then incubated in 3% H_20_2 to quench endogenous peroxidase activity. Sections were then blocked in species-specific normal sera for 30–60 min to reduce nonspecific staining, and subsequently incubated with primary antibodies followed by a biotinylated secondary antibody. The immunostaining was detected with peroxidase-conjugated streptavidin using diaminobenzidine as chromagen (VECTASTAIN Elite ABC Kit, Vector).

Cell Proliferation and Apoptosis Assays

Cell proliferation was measured by IHC of PCNA or BrdU incorporation assays. For BrdU incorporation, mice were injected intraperitoneally with BrdU (10 μl/g body weight). After 2 hr, testis specimens were collected, preserved overnight in 10% neutral buffered formalin, and embedded in paraffin. Sections (4–6 μm) were cut and deparaffinized in xylene and rehydrated in descending ethanol series. BrdU incorporation was detected using BrdU IHC System (Zymed Laboratories). Apoptotic cells were detected by TUNEL assay using the ApopTag Peroxidase In Situ Apoptosis Detection Kit (Chemicon International) or by IHC using Cleaved Caspase-3 antibody (Cell Signaling, Boston, MA) along with Vectorstain Elite ABC Kit (Vector Laboratories, Burlingame, CA).

Germ Cell Preparation DNA Content Analysis

Testicular cell preparation and DNA content analysis were as described (Russell et al., 2002). Briefly, seminiferous tubules were dissected from testes and placed in PBS in a conical tube. The tubules were allowed to settle and excess PBS was removed before digestion with 0.25% (wt/vol) collagenase (GIBCO) for 15–30 min at 32°C. The tubules were washed with PBS, digested in 25% (wt/vol) trypsin with 1 μg/ml DNase (Roche) for 10–20 min at 32°C, and then the reaction was aborted by adding FBS to a final concentration of 10% (vol/vol). Single cell suspension was filtered through a cell strainer (BD Falcon) and collected for experiments.

For DNA content analyses, germ cell suspensions were harvested by centrifugation, washed in PBS, and fixed in 70% ethanol for at least 1 hr (or overnight) at 4°C. The cells were washed twice in PBS, resuspended in 500 μl of propidium iodide (Sigma) solution (0.1% v/v Triton-X, 50 μg/ml RNaseA, 25 μg/ml propidium iodide) for 30 min at room temperature or overnight at 4°C, and then analyzed by flow cytometry.

IB, EMSA, and In Vitro Kinase Assays

Germ cells were lysed in a kinase cell lysis buffer and subjected to in vitro kinase assays and IB (Uhlik et al., 1998). Nuclear extracts were prepared and subjected to EMSA using a ^{32}P-radiolabeled κB probe or a control NF-Y probe (Wu and Sun, 2007). Antibody supershift and DNA competition assays were performed as described (Sun et al., 1998).

Ubiquitination Assays

RIP1 was isolated from germ cells by IP, and the ubiquitinated RIP1 was detected by IB using anti-ubiquitin. For the transfection model, 293T or HeLa cells were transfected in 12-well plates and either left untreated (293T cells) or stimulated with TNF-α for 2 min (HeLa cells). RIP1 was isolated by IP using anti-Flag followed by detecting ubiquitinated RIP1 by IB using anti-HA-HRP.

Real-Time Quantitative PCR

Total RNA was isolated from germ cells using TRI reagent (Molecular Research Center, Inc.) and subjected to cDNA synthesis using RNase H-reverse transcriptase (Invitrogen) and oligo (dT) primers. The initial quantity of cDNA samples was calculated from primer-specific standard curves with iCycler Data Analysis software. Real-time quantitative PCR was performed using iCycler Sequence Detection System (Bio-Rad) and RT^2 Real-Time™ SYBR green PCR master mix (Superarray). The expression of individual genes was calculated by a standard curve method and normalized to the expression of L32. Data are presented as fold change between the wild-type and *Cyld*$^{-/-}$ cells. The gene-specific primer sets were: IκBα, 5′-CTGCAGGCCACCAACTACAA-3′ and 5′-CAGCACCCAAAGTCACCAAGT-3′; Bcl-XL, 5′-TCTGAATGA CCACCTAGAGC-3′ and 5′-GGTCAGTGTCTGGTCACTTC-3′; L32, 5′-AAGCGAAACTGGCGGAAA-C3′and 5′-TAACCGATGTTGGGCAT CAG-3′; c-IAP1, 5′-CCTTCTAGTGCACTAGTTCA-3′ and 5′-CTTGA CATCATCACTGTGTC-3′; 5′-AAGACAGACTGAAGAGATGG-3′; c-IAP2, 5′-AGGACATGTGTCAACTGTTG-3′ and 5′-AGGACATGTGTCAACT GTTG-3′.

Statistics

Statistical significance was determined by t test.

Supplemental Data

Supplemental Data include seven figures and can be found with this article online at http://www.developmentalcell.com/cgi/content/full/13/5/705/DC1/.

ACKNOWLEDGMENTS

We thank Kang Li and Nate Sheaffer of the Pennsylvania State College of Medicine Core facilities for assistance with tissue sections and flow cytometry, Dr. Collin J. Barnstable for help in microscopy, and Dr. Laurence Demers for serum testosterone analysis. We also thank Vincent Chau, Zhijian Chen, Barbara Miller, and Margaret Offermann for reagents. This study was supported by grants from National Institutes of Health (AI064639 and CA94922 to S.C.S., AI057555 to S.C.S. and M.Z.). A.W. is a recipient of the Ruth L. Kirschstein National Research Service Award.

Received: February 7, 2007
Revised: July 9, 2007
Accepted: September 13, 2007
Published: November 5, 2007

REFERENCES

Bignell, G.R., Warren, W., Seal, S., Takahashi, M., Rapley, E., Barfoot, R., Green, H., Brown, C., Biggs, P.J., Lakhani, S.R., et al. (2000). Identification of the familial cylindromatosis tumour-suppressor gene. Nat. Genet. *25*, 160–165.

Brummelkamp, T.R., Nijman, S.M., Dirac, A.M., and Bernards, R. (2003). Loss of the cylindromatosis tumour suppressor inhibits apoptosis by activating NF-κB. Nature *424*, 797–801.

Catz, S.D., and Johnson, J.L. (2001). Transcriptional regulation of bcl-2 by nuclear factor κB and its significance in prostate cancer. Oncogene *20*, 7342–7351.

Chen, Z.J. (2005). Ubiquitin signalling in the NF-κB pathway. Nat. Cell Biol. *7*, 758–765.

Coultas, L., Bouillet, P., Loveland, K.L., Meachem, S., Perlman, H., Adams, J.M., and Strasser, A. (2005). Concomitant loss of proapoptotic BH3-only Bcl-2 antagonists Bik and Bim arrests spermatogenesis. EMBO J. *24*, 3963–3973.

De, S.K., Chen, H.L., Pace, J.L., Hunt, J.S., Terranova, P.F., and Enders, G.C. (1993). Expression of tumor necrosis factor-α in mouse spermatogenic cells. Endocrinology *133*, 389–396.

de Kretser, D.M., Loveland, K.L., Meinhardt, A., Simorangkir, D., and Wreford, N. (1998). Spermatogenesis. Hum. Reprod. *13* (*Suppl 1*), 1–8.

Ea, C.K., Deng, L., Xia, Z.P., Pineda, G., and Chen, Z.J. (2006). Activation of IKK by TNFα requires site-specific ubiquitination of RIP1 and polyubiquitin binding by NEMO. Mol. Cell *22*, 245–257.

Feuillard, J., Schuhmacher, M., Kohanna, S., Asso-Bonnet, M., Ledeur, F., Joubert-Caron, R., Bissieres, P., Polack, A., Bornkamm, G.W., and Raphael, M. (2000). Inducible loss of NF-κB activity is associated with apoptosis and Bcl-2 down-regulation in Epstein-Barr virus-transformed B lymphocytes. Blood *95*, 2068–2075.

Furuchi, T., Masuko, K., Nishimune, Y., Obinata, M., and Matsui, Y. (1996). Inhibition of testicular germ cell apoptosis and differentiation in mice misexpressing Bcl-2 in spermatogonia. Development *122*, 1703–1709.

Gavrieli, Y., Sherman, Y., and Ben-Sasson, S.A. (1992). Identification of programmed cell death in situ via specific labeling of nuclear DNA fragmentation. J. Cell Biol. *119*, 493–501.

Haglund, K., and Dikic, I. (2005). Ubiquitylation and cell signaling. EMBO J. *24*, 3353–3359.

Kaiser, W.J., and Offermann, M.K. (2005). Apoptosis induced by the toll-like receptor adaptor TRIF is dependent on its receptor interacting protein homotypic interaction motif. J. Immunol. *174*, 4942–4952.

Karin, M., and Lin, A. (2002). NF-κB at the crossroads of life and death. Nat. Immunol. *3*, 221–227.

Knudson, C.M., Tung, K.S., Tourtellotte, W.G., Brown, G.A., and Korsmeyer, S.J. (1995). Bax-deficient mice with lymphoid hyperplasia and male germ cell death. Science *270*, 96–99.

Kovalenko, A., Chable-Bessia, C., Cantarella, G., Israel, A., Wallach, D., and Courtois, G. (2003). The tumour suppressor CYLD negatively regulates NF-κB signalling by deubiquitination. Nature *424*, 801–805.

Li, H., Kobayashi, M., Blonska, M., You, Y., and Lin, X. (2006). Ubiquitination of RIP is required for tumor necrosis factor α-induced NF-κB activation. J. Biol. Chem. *281*, 13636–13643.

Lim, J.H., Stirling, B., Derry, J., Koga, T., Jono, H., Woo, C.H., Xu, H., Bourne, P., Ha, U.H., Ishinaga, H., et al. (2007). Tumor suppressor CYLD regulates acute lung injury in lethal *Streptococcus pneumoniae*. Infect. Immun. *27*, 349–360.

Malkov, M., Fisher, Y., and Don, J. (1998). Developmental schedule of the postnatal rat testis determined by flow cytometry. Biol. Reprod. *59*, 84–92.

Massoumi, R., Chmielarska, K., Hennecke, K., Pfeifer, A., and Fassler, R. (2006). Cyld inhibits tumor cell proliferation by blocking bcl-3-dependent NF-κB signaling. Cell *125*, 665–677.

McCarrey, J.R. (1993). Development of the germ cell. In Cell and Molecular Biology of the Testis, C. Desjardins and L.L. Ewing, eds. (New York: Oxford University Press Inc.), pp. 58–89.

Mori, C., Nakamura, N., Dix, D.J., Fujioka, M., Nakagawa, S., Shiota, K., and Eddy, E.M. (1997). Morphological analysis of germ cell apoptosis during postnatal testis development in normal and Hsp 70–2 knockout mice. Dev. Dyn. *208*, 125–136.

Nebel, B.R., Amarose, A.P., and Hacket, E.M. (1961). Calendar of gametogenic development in the prepuberal male mouse. Science *134*, 832–833.

Nijman, S.M., Luna-Vargas, M.P., Velds, A., Brummelkamp, T.R., Dirac, A.M., Sixma, T.K., and Bernards, R. (2005). A genomic and functional inventory of deubiquitinating enzymes. Cell *123*, 773–786.

Print, C.G., and Loveland, K.L. (2000). Germ cell suicide: new insights into apoptosis during spermatogenesis. Bioessays *22*, 423–430.

Print, C.G., Loveland, K.L., Gibson, L., Meehan, T., Stylianou, A., Wreford, N., de Kretser, D., Metcalf, D., Kontgen, F., Adams, J.M., et al. (1998). Apoptosis regulator bcl-w is essential for spermatogenesis but appears otherwise redundant. Proc. Natl. Acad. Sci. USA *95*, 12424–12431.

Reiley, W., Zhang, M., and Sun, S.-C. (2004). Tumor suppressor negatively regulates JNK signaling pathway downstream of TNFR members. J. Biol. Chem. *279*, 55161–55167.

Reiley, W., Zhang, M., Wu, X., Graner, E., and Sun, S.-C. (2005). Regulation of the deubiquitinating enzyme CYLD by IκB kinase γ-dependent phosphorylation. Mol. Cell. Biol. *25*, 3886–3895.

Reiley, W.W., Zhang, M., Jin, W., Losiewicz, M., Donohue, K.B., Norbury, C.C., and Sun, S.C. (2006). Regulation of T cell development by the deubiquitinating enzyme CYLD. Nat. Immunol. *7*, 411–417.

Reiley, W.W., Jin, W., Lee, A.J., Wright, A., Wu, X., Tewalt, E.F., Leonard, T.O., Norbury, C.C., Fitzpatrick, L., Zhang, M., et al. (2007). Deubiquitinating enzyme CYLD negatively regulates the ubiquitin-dependent kinase Tak1 and prevents abnormal T cell responses. J. Exp. Med. *204*, 1475–1485.

Rodriguez, I., Ody, C., Araki, K., Garcia, I., and Vassalli, P. (1997). An early and massive wave of germinal cell apoptosis is required for the development of functional spermatogenesis. EMBO J. *16*, 2262–2270.

Russell, L.D., Chiarini-Garcia, H., Korsmeyer, S.J., and Knudson, C.M. (2002). Bax-dependent spermatogonia apoptosis is required for testicular development and spermatogenesis. Biol. Reprod. *66*, 950–958.

Sun, S.-C., Ganchi, P.A., Ballard, D.W., and Greene, W.C. (1993). NF-κB controls expression of inhibitor IκBα: evidence for an inducible autoregulatory pathway. Science *259*, 1912–1915.

Sun, S.-C., Maggirwar, S.B., Harhaj, E.W., and Uhlik, M. (1998). Binding of c-Rel to STAT5 target sequences in HTLV-I-transformed T cells. Oncogene *18*, 1401–1409.

Suominen, J.S., Wang, Y., Kaipia, A., and Toppari, J. (2004). Tumor necrosis factor-α (TNF-α) promotes cell survival during spermatogenesis, and this effect can be blocked by infliximab, a TNF-α antagonist. Eur. J. Endocrinol. *151*, 629–640.

Trompouki, E., Hatzivassiliou, E., Tsichritzis, T., Farmer, H., Ashworth, A., and Mosialos, G. (2003). CYLD is a deubiquitinating enzyme that negatively regulates NF-κB activation by TNFR family members. Nature *424*, 793–796.

Uhlik, M., Good, L., Xiao, G., Harhaj, E.W., Zandi, E., Karin, M., and Sun, S.-C. (1998). NF-κB-inducing kinase and IκB kinase participate in human T-cell leukemia virus I Tax-mediated NF-κB activation. J. Biol. Chem. *273*, 21132–21136.

Wu, X., and Sun, S.C. (2007). Retroviral oncoprotein Tax deregulates NF-κB by activating Tak1 and mediating Tak1-IKK physical association. EMBO Rep. *8*, 510–515.

Wu, C.J., Conze, D.B., Li, T., Srinivasula, S.M., and Ashwell, J.D. (2006). Sensing of Lys 63-linked polyubiquitination by NEMO is a key event in NF-κB activation. Nat. Cell Biol. *8*, 398–406.

Zhang, J., Stirling, B., Temmerman, S.T., Ma, C.A., Fuss, I.J., Derry, J.M., and Jain, A. (2006). Impaired regulation of NF-κB and increased susceptibility to colitis-associated tumorigenesis in CYLD-deficient mice. J. Clin. Invest. *116*, 3042–3049.